NOTES AND CORRESPONDENCE

A Simple Model for Random Wave Bottom Friction and Dissipation

QINGPING ZOU

Department of Oceanography, Dalhousie University, Halifax, Nova Scotia, Canada

6 May 2002 and 24 November 2003

ABSTRACT

Based on the spectral eddy viscosity model of bottom boundary layers, the spectral representation of bottom friction and dissipation for irregular waves is reduced to an equivalent monochromatic wave representation. The representative wave amplitude and frequency are chosen so that the bottom velocity and bottom shear stress variances of the equivalent wave model are identical to those of the spectral model. Moreover, these variances have to satisfy the same relationship as those of a monochromatic wave with the same frequency. According to the wave bottom boundary layer theory, the ratio between bottom stress spectrum and bottom velocity spectrum has a frequency dependence of ω^q, where the exponent q is a positive constant. The representative wave frequency and direction are obtained based on this power law, whereas in previous studies they were derived using a Taylor expansion of the ratio about a particular frequency or were proposed heuristically. Previous equivalent wave theories are therefore valid only for narrowbanded wave spectra. The present theory, however, is applicable to a wide variety of wave spectra including broadbanded and multimodal spectra.

1. Introduction

Energy dissipation of random ocean waves due to bottom friction was first addressed explicitly by Hasselmann and Collins (1968) and then modified by Collins (1972). They used a quadratic drag law to relate the bottom shear stress to the wave bottom velocity and assumed a constant drag coefficient and zero phase shift between these two variables. More recently, eddy viscosity models were applied to this problem by Madsen et al. (1988) and Weber (1991a,b). The former used an equivalent monochromatic wave representation of the bottom friction and dissipation induced by the random wave forcing, while the latter used a spectral representation. The eddy viscosity models are different from the quadratic drag law because they relate the bottom shear stress to the bottom velocity by a complex transfer function that is dependent on the bottom roughness and frequency. This gives rise to a nonzero phase shift between the bottom stress and velocity. The equivalent wave approach by Madsen et al. (1988) is more straight forward and efficient and therefore has been adopted by Tolman (1994), Young and Gorman (1995), and Ardhuin et al. (2001) in their wave forecast and hindcast models.

Most recently, the equivalent wave technique was employed by Madsen (1994) to study spectral wave–current bottom boundary layers, which are commonly found on the continental shelf and near-shore region. Because of its direct influence on sediment transport, many theoretical and numerical studies have considered this problem in the past decade. Simple models such as those by Grant and Madsen (1979) and Christoffersen and Jonsson (1985) were found to agree reasonably well with more complicated numerical models. In order to apply these simple models to irregular waves, however, one has to first define the characteristics of the equivalent monochromatic wave such as the representative bottom velocity amplitude u_{wr}, frequency ω_r, and direction θ_{wr} (Mathisen and Madsen 1999; Madsen 1994).

The following representative frequencies have been used previously in the studies of bottom friction and dissipation of irregular waves:

$$\omega_r = \omega_p, \tag{1.1}$$

where ω_p is the wave peak frequency (Weber 1991a,b),

$$\omega_r \equiv \omega_{rq} = \left[\frac{\iint \omega^q S_{u_w}(\omega, \theta)\, d\omega\, d\theta}{\iint S_{u_w}(\omega, 0)\, d\omega\, d\theta} \right]^{1/q}, \tag{1.2}$$

where $q = 1$ is used by Madsen (1994) and $q = -2$ is used by Madsen et al. (1988), Tolman (1994), and Ardhuin et al. (2001); $S_{u_w}(\omega, \theta)$ is the directional spectrum of the wave bottom velocity. These formulas result in

Corresponding author address: Dr. Qingping Zou, Department of Oceanography, Dalhousie University, Halifax, NS B3H 4J1, Canada. E-mail: qingping@phys.ocean.dal.ca

differing representative frequency for differing $S_{u_w}(\omega, \theta)$ conditions, unless the wave bottom velocity spectrum is extremely narrow—that is, $S_{u_w}(\omega, \theta) \approx S_{u_w}(\omega_r, \theta)\delta(\omega - \omega_r)$, where δ is the Dirac delta function.

The above definitions of representative frequency were proposed heuristically, except for (1.2) with $q = 1$ by Madsen (1994). Assuming narrowbanded bottom velocity spectra and using the Taylor expansion of the transfer function between bottom stress and velocity about a particular frequency, Madsen (1994) obtained $q = 1$ regardless of the transfer function. It was conjectured that a full spectral analysis should be used for broadbanded wave spectra (Weber 1991b).

The primary objective of this study is to extend the equivalent wave theory of Madsen (1994) to broadbanded wave spectra. The characteristics of the equivalent wave formulation are rederived from the spectral eddy viscosity model of bottom boundary layers for waves with arbitrary spectral shape and bottom roughness. Comparisons among the present and previous equivalent wave models and spectral models are conducted for these cases.

2. Theory

a. Equivalent wave model

We consider here the wave bottom boundary layer beneath an irregular wave with a bottom velocity spectrum of $S_{u_w}(\omega, \theta)$. The bottom stress spectrum relates to the bottom velocity spectrum by [see (13) of Madsen 1994]

$$S_{\tau_w}(\omega, \theta) = \{\kappa u_{*_r}|T[\zeta_0(\omega)]|\}^2 S_{u_w}(\omega, \theta), \quad (2.1)$$

where

$$T[\zeta_0(\omega)] = \frac{\sqrt{i\zeta_0(\omega)}K_1[2\sqrt{i\zeta_0(\omega)}]}{K_0[2\sqrt{i\zeta_0(\omega)}]}, \quad (2.2)$$

$\zeta_0(\omega) = \omega z_0/\kappa u_{*r}$, $\kappa = 0.4$ is von Kármán's constant, $z_0 = r/30$, r is the Nikuradse roughness length, u_{*r} is a priori unknown friction velocity, and K_0 and K_1 are the zeroth- and first-order modified Bessel functions.

We then propose the following two criteria for the equivalent wave. First, the bottom velocity and bottom shear stress variances of the equivalent wave must be the same as those of the spectral model, where they are related to each other by the same transfer function as for a monochromatic wave, that is, the representative wave. Thus, the representative velocity amplitude is

$$u_{wr}^2 = 2\iint S_{u_w}(\omega, \theta)\, d\omega\, d\theta. \quad (2.3)$$

The representative frequency ω_r must satisfy the relationship of

$$|T[\zeta_0(\omega_r)]|^2 = \frac{\iint |T[\zeta_0(\omega)]|^2 S_{u_w}(\omega, \theta)\, d\omega\, d\theta}{\iint S_{u_w}(\omega, \theta)\, d\omega\, d\theta}. \quad (2.4)$$

Second, the representative direction θ_{wr} must be coincident with the vector mean direction of the bottom shear stress; that is,

$$\theta_{wr} = \tan^{-1}\frac{\iint S_{\tau_w}(\omega, \theta)\sin\theta\, d\omega\, d\theta}{\iint S_{\tau_w}(\omega, \theta)\cos\theta\, d\omega\, d\theta}. \quad (2.5)$$

Invoking the following approximation of $T(\zeta_0)$ (see the appendix),

$$|T(\zeta_0)|^2 = C_\zeta \zeta_0^q, \quad (2.6)$$

where C_ζ is a constant coefficient,

$$q = 0.75 + 0.15\log_{10}\frac{r}{A_r}, \quad \text{for } \frac{r}{A_r} \geq 10^{-3}, \quad \text{and} \quad (2.7)$$

$$q = 0.6 + 0.088\log_{10}\frac{r}{A_r}, \quad \text{for } \frac{r}{A_r} \leq 10^{-3} \quad (2.8)$$

($A_r = U_{wr}/\omega_r$ is the representative wave orbital amplitude), we reduce (2.4) and (2.5) to

$$\omega_r = \left[\frac{\iint \omega^q S_{u_w}(\omega, \theta)\, d\omega\, d\theta}{\iint S_{u_w}(\omega, \theta)\, d\omega\, d\theta}\right]^{1/q} \quad \text{and} \quad (2.9)$$

$$\theta_{wr} = \tan^{-1}\frac{\iint \omega^q S_{u_w}(\omega, \theta)\sin\theta\, d\omega\, d\theta}{\iint \omega^q S_{u_w}(\omega, \theta)\cos\theta\, d\omega\, d\theta}. \quad (2.10)$$

Although the present definition of representative frequency in (2.9) takes the same form as those of previous studies [(1.2)], the exponent q given by (2.7) and (2.8) is different from $q = 1$ by Madsen (1994), $q = -1$ by Weber (1991a), and $q = -2$ by Madsen et al. (1988), Tolman (1994), and Ardhuin et al. (2001). As demonstrated in the next section, in case of multidirectional waves, the present representative direction also deviates from that of Madsen (1994), who assumed that the representative direction is the same as the vector mean direction of wave bottom velocity

$$\theta_{wm} = \tan^{-1}\frac{\iint S_{u_w}(\omega, \theta)\sin\theta\, d\omega\, d\theta}{\iint S_{u_w}(\omega, \theta)\cos\theta\, d\omega\, d\theta}. \quad (2.11)$$

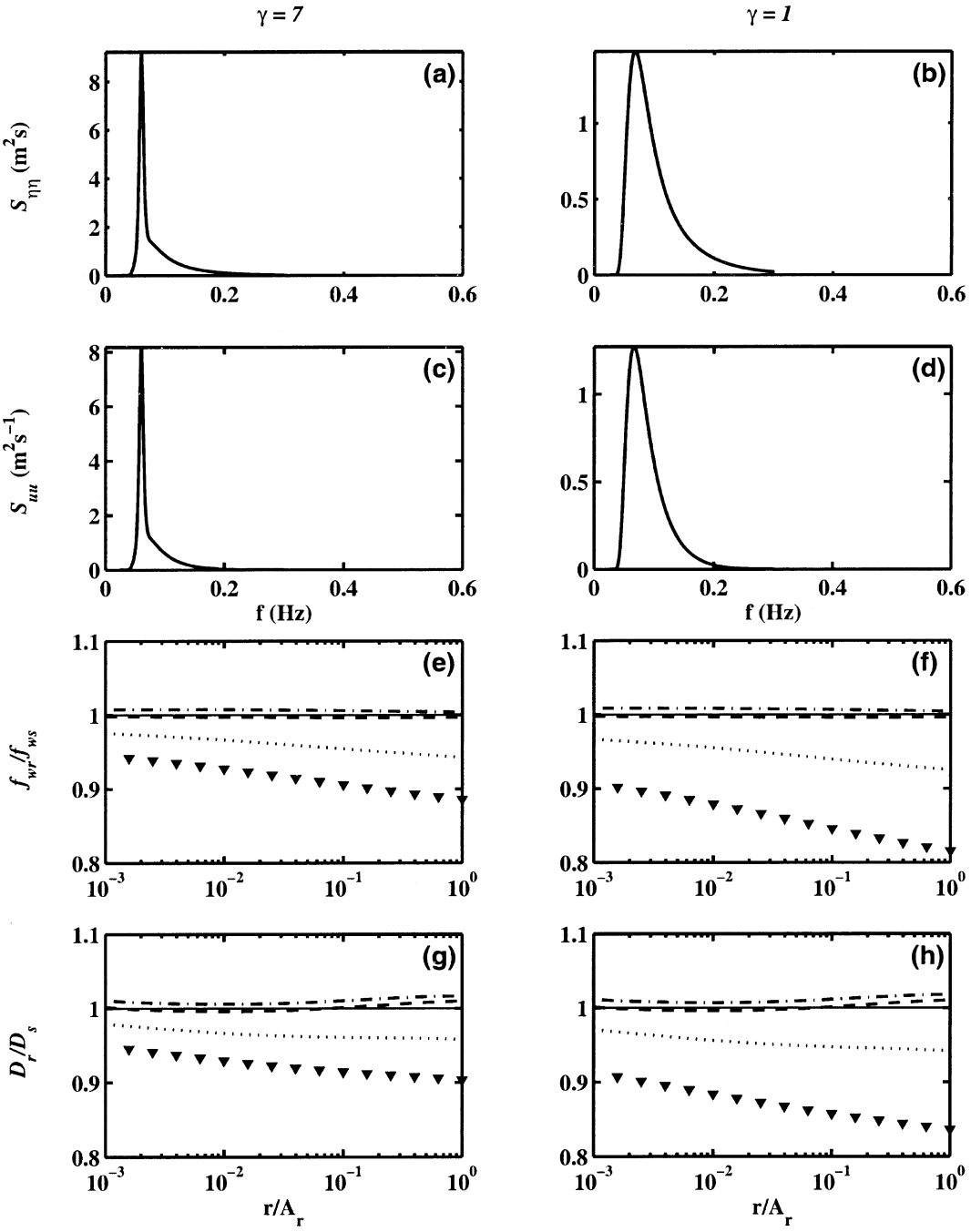

FIG. 1. (e), (f) Friction factor f_{wr} and (g), (h) total bottom dissipation D_r, predicted by the present and previous equivalent wave models, normalized by the spectral model predictions f_{ws} and D_s, as a function of the relative bottom roughness r/A_r, for a unimodal wave at a 10-m water depth using a JONSWAP-type spectrum with a peak enhancement parameter of (left) $\gamma = 7$ and (right) $\gamma = 1$, a peak frequency of $f_p = 0.06$ Hz, a Phillips coefficient $\alpha = 0.005$, and a spectral bandwidth parameter $\sigma = 0.08$. (a), (b) Surface elevation spectra and (c), (d) bottom velocity spectra. Spectral model (solid lines); present equivalent wave model with $\omega_r = \omega_{rq}$ [(1.2), (2.7), and (2.8)] (dashed lines); previous models with $\omega_r = \omega_p$ [(1.1)] (downward triangles), $\omega_r = \omega_{r1}$, [(1.2)] (dash–dot lines), and $\omega_r = \omega_{r-2}$ [(1.2)] (dotted lines).

The sensitivity of the wave bottom friction and dissipation relative to q will be examined in the next section.

b. Bottom friction and dissipation

To further simplify the evaluation of the wave bottom friction and dissipation, we adopted the explicit formulas of the friction factor proposed by Madsen (1994)

$$f_{wr} = \exp\left[7.02\left(\frac{r}{A_r}\right)^{0.078} - 8.82\right], \quad \text{for } 10^{-2} < \frac{r}{A_r} < 5, \quad \text{and} \tag{2.12}$$

$$f_{wr} = \exp\left[5.61\left(\frac{r}{A_r}\right)^{0.109} - 7.30\right], \quad \text{for } 10^{-4} < \frac{r}{A_r} < 10^{-2}, \tag{2.13}$$

which have 1% accuracy in comparison with the exact implicit formula.

We also adopted the explicit formulas for the phase lead of the wave bottom shear stress relative to the wave bottom velocity, proposed by Madsen (1994):

$$\theta_T^r = 33 + 6.0 \log_{10}\frac{r}{A_r}, \quad \text{for } \frac{r}{A_r} \geq 4 \times 10^{-3}, \tag{2.14}$$

and

$$\theta_T^r = 25 + 3.4 \log_{10}\frac{r}{A_r}, \quad \text{for } \frac{r}{A_r} \leq 4 \times 10^{-3}, \tag{2.15}$$

which has an error of less than 1°.

Following Kajiura (1968) and Weber (1991b), the wave bottom dissipation is given by

$$D = \iint D(\omega, \theta)\, d\omega\, d\theta, \tag{2.16}$$

where

$$D(\omega, \theta) = C_D(\omega) S_{u_w}(\omega, \theta) \tag{2.17}$$

is the spectral wave dissipation,

$$C_D(\omega) = \kappa u_{*_r} |T[\zeta_0(\omega)]| \cos[\theta_T(\omega)] \tag{2.18}$$

is the wave energy dissipation coefficient, and θ_T is the phase of the complex transfer function $T[\zeta_0(\omega)]$.

Substituting ω with ω_r and invoking (2.3) reduces (2.16) to the equivalent wave representation of the bottom dissipation

$$D_r = \frac{1}{2}\kappa u_{*_r} |T[\zeta_0(\omega_r)]| \cos\theta_T^r u_{wr}^2. \tag{2.19}$$

Further substitution of (A.1) and $u_{*wr}^2 \equiv f_{wr} u_{wr}^2/2$ into (2.19) yields

$$D_r = \frac{1}{4} f_{wr} \cos\theta_T^r u_{wr}^3, \tag{2.20}$$

where f_{wr} and θ_T^r are given explicitly by (2.12), (2.13), and (2.14), respectively.

TABLE 1. Wave peak frequency f_p, peak wavenumber k_p, rms surface elevation η_{rms}, and bottom velocity u_{rms} for a unimodal wave A (see Fig. 1a) and B (see Fig. 1b) at a water depth of 10 m.

	f_p (Hz)	k_p (m^{-1})	η_{rms} (m)	u_{rms} (m s^{-1})
Unimodal wave A	0.06	0.039	0.41	0.36
Unimodal wave B	0.06	0.039	0.32	0.26

3. Comparisons of spectral and equivalent wave models

a. Bottom friction and dissipation of unimodal and bimodal waves

The finite-depth Joint North Sea Wave Project (JONSWAP) spectrum proposed by Graber (1984) and Bouws et al. (1985), also known as the TMA spectrum, is adopted here to construct unimodal and bimodal wave spectra whose bottom velocity spectra take the form of

$$S_{u_w}(\omega) = \left(\frac{\omega}{\sinh kh}\right)^2 \sum_{i=1}^{m} \beta_i E_{\text{TMA}}(\omega, \omega_{pi}, h, \alpha, \gamma, \sigma), \tag{3.1}$$

where $m = 1$ and 2 represent unimodal and bimodal spectra, E_{TMA} is the finite-depth JONSWAP spectrum, ω_{pi} are the wave peak frequencies, h is the water depth, α is the Phillips coefficient, γ is the peak enhancement parameter, σ is the bandwidth parameter, and β_i is the spectral energy weight coefficient. For unimodal waves, $\beta_1 = 1$. For bimodal waves, β_1 and β_2 are chosen so that the significant wave height for the wind sea spectrum at the high frequency is one-quarter of the water depth and that $S_{u_w}(\omega_{p2})/S_{u_w}(\omega_{p1}) = \omega_{p1}/\omega_{p2}$ and both the spectral peaks have comparable contributions to the bottom shear stress.

The friction factor and total wave dissipation predicted by the present and previous equivalent wave models, f_{wr} and D_r, are compared with those of the spectral model, f_{ws} and D_s, in Fig. 1 for a unidirectional unimodal JONSWAP wave spectrum described in Table 1. As shown in Fig. 1, both the present equivalent wave theory and that of Madsen (1994) are in good agreement with the spectral model. By comparison, the model of Madsen et al. (1988), using $\omega_r = \omega_{r-2}$, and Weber (1991a,b), using $\omega_r = \omega_{p1}$ and $\omega_r = \omega_{p2}$, deviate from the spectral model with a relative errors up to 10% and 20%, respectively.

As indicated by Fig. 2, the present equivalent wave theory is able to reproduce the spectral model results for the bimodal wave spectra described by Table 2. Although the Madsen (1994) model gives a slightly larger relative error of 5%, it is still in reasonable agreement

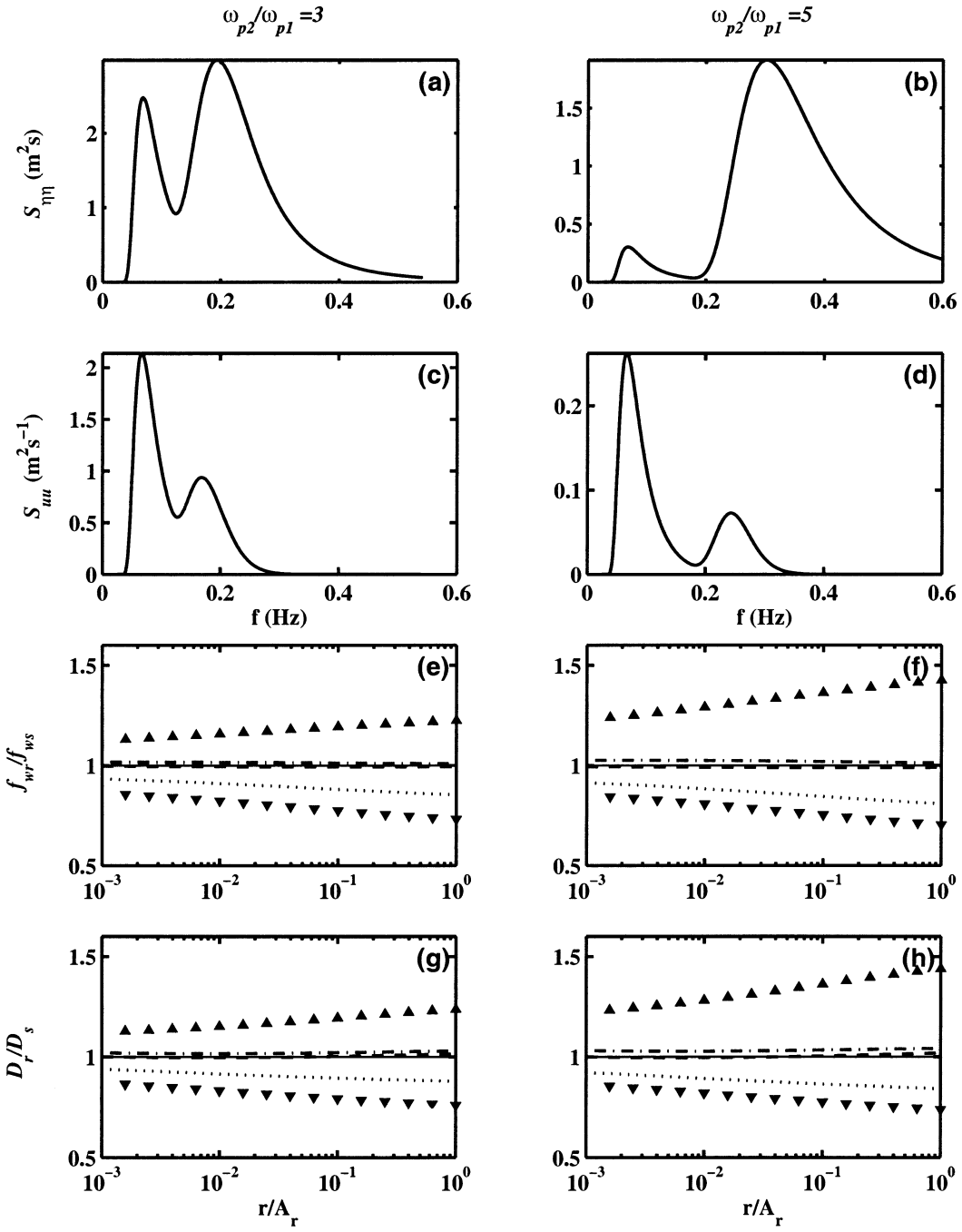

FIG. 2. Same as Fig. 1, but for a bimodal wave with a JONSWAP-type spectrum with a wave peak frequency ratio of (left) $\omega_{p2}/\omega_{p1} = 3$ and (right) $\omega_{p2}/\omega_{p1} = 5$, a Phillips coefficient $\alpha = 0.001$, and a peak enhancement parameter of $\gamma = 1$; predictions of the equivalent wave models using the representative frequency $\omega_r = \omega_{p2}$ [(1.1)] (upward triangles) and $\omega_r = \omega_{p1}$ [(1.1)] (downward triangles).

with the spectral model. However, the equivalent wave models using $\omega_r = \omega_{r-2}$ (Madsen et al. 1988) and $\omega_r = \omega_{p1}$ and $\omega_r = \omega_{p2}$ (Weber 1991a,b) deviate from the spectral model by 20% and 40%, respectively. The deviations increase with relative roughness as the result of increasing difference between previous and present values of q.

Given a relative roughness of 0.1, Fig. 3 illustrates the bottom friction and dissipation predicted by the present and previous equivalent wave theory and spectral model for bimodal waves with a range of spectral width. The deviations of the present theory and Madsen's (1994) from the spectral model increase slightly with the spectral width, whereas the deviations of the pre-

TABLE 2. Wave peak frequency f_p, peak wavenumber k_p, rms surface elevation η_{rms}, and bottom velocity u_{rms} for the sea and swell components of a bimodal wave A (see Fig. 2a) and B (see Fig. 2b) at a water depth of 10 m.

	f_p (Hz)	k_p (m^{-1})	η_{rms} (m)	u_{rms} (m s^{-1})
Bimodal wave A (swell)	0.06	0.039	0.42	0.35
Bimodal wave A (sea)	0.18	0.15	0.63	0.25
Bimodal wave A (swell + sea)			0.75	0.43
Bimodal wave B (swell)	0.06	0.039	0.15	0.12
Bimodal wave B (sea)	0.30	0.36	0.63	0.073
Bimodal wave B (swell + sea)			0.64	0.14

vious theory using $\omega_r = \omega_{r-2}$ (Madsen et al. 1988) and $\omega_r = \omega_{p1}$ and $\omega_r = \omega_{p2}$ (Weber 1991a,b) from the spectral model increase considerably with the spectral bandwidth. Following Longuet-Higgins (1983), we used

$$\upsilon^2 = \frac{\iint (\omega - \omega_r)^2 S_{u_b}(\omega, \theta)\, d\omega\, d\theta}{\iint \omega_r^2 S_{u_b}(\omega, \theta)\, d\omega\, d\theta} \tag{3.2}$$

to characterize the spectral bandwidth.

b. Representative direction

To verify the representative direction θ_{wr} given by (2.10) against that suggested by the spectral model, we constructed a directional bottom velocity spectrum by multiplying that of a unidirectional bimodal wave [(3.1)] (see also Fig. 2a and Table 1) with a direction spreading function; that is,

$$S_{u_w}(\omega, \theta) = \left(\frac{\omega}{\sinh kh}\right)^2 \sum_{i=1}^{m} \beta_i E_{\text{TMA}}(\omega, \omega_{pi}, h, \alpha, \gamma, \sigma) \times \cos[0.5(\theta - \theta_i)^s], \tag{3.3}$$

where $s = 20$ is the directional spreading parameter, and θ_i is the dominant wave direction. The present representative wave direction is consistent with that of the spectral model (Fig. 4). However, both deviate significantly from the representative wave direction proposed by Madsen (1994) in his study of wave–current interactions, which is assumed to be the same as the vector mean direction of the wave bottom velocity. The effects of wave direction and currents on the wave bottom friction are significant for current-dominant situations but not for wave-dominant situations that are often found in the continental shelf region (Fig. 5).

4. Summary and discussion

Based on a spectral eddy viscosity model of bottom boundary layers, we have derived an equivalent monochromatic wave representation of bottom friction and dissipation for irregular waves. According to the wave bottom boundary layer theory, the ratio between bottom stress spectrum and bottom velocity spectrum has a frequency dependence of ω^q where the exponent q is a positive constant. The bottom stress variance is therefore proportional to $\iint \omega^q S_{u_w}(\omega, \theta)\, d\omega\, d\theta$. In order to conserve the bottom stress and bottom velocity variances, the representative frequency ω_r of the equivalent wave has to satisfy the relationship $\iint \omega_r^q S_{u_w}(\omega, \theta)\, d\omega\, d\theta = \iint \omega^q S_{u_w}(\omega, \theta)\, d\omega\, d\theta$. From the vector mean direction of the bottom shear stress, the representative direction of the equivalent wave is reduced to

$$\theta_{wr} = \tan^{-1} \frac{\iint \omega^q S_{u_w}(\omega, \theta) \sin\theta\, d\omega\, d\theta}{\iint \omega^q S_{u_w}(\omega, \theta) \cos\theta\, d\omega\, d\theta}.$$

We found that the exponent q increases from 0.25 to 0.75 as the relative bottom roughness increases from 10^{-4} to 10^{0}. This is consistent with the previous findings that the slope of friction factor versus relative roughness is 0.25 and 0.75 for a relative roughness smaller and larger than 0.02 (Kamphuis 1974; Fredsoe and Deigard 1992). The positive values of q reflect the fact that the wave boundary layer thickness is inversely proportional to the wave frequency. Therefore, a stronger velocity shear is induced by a high-frequency wave component at the bottom, which generates a larger bottom shear stress.

By comparison, $q = 1$ was obtained by Madsen (1994) from the Taylor expansion of the transfer function about a particular frequency, regardless of the transfer function. Since $q = 1$ closely approximates the present value of q, both theories are in good agreement with the spectral model for the unimodal and bimodal waves (Figs. 1 and 2). Despite that, only the present theory provides the valid interpretation for the equivalent wave presentation of broadbanded and multimodal wave spectra. $q = -2$ by Madsen et al. (1988), Tolman (1994), and Ardhuin et al. (2001) as well as the wave peak frequency by Weber (1991a,b) result in bottom friction and dissipation that is in a reasonable agreement with those of the spectral model for the narrowbanded spectra (Fig. 1) but deviate significantly from those of the spectral model for the bimodal wave spectra (Fig. 2). The narrow and single-peaked bottom velocity spectra occur when the wind is homogeneous and stationary and in moderate finite depth. The broad and bimodal

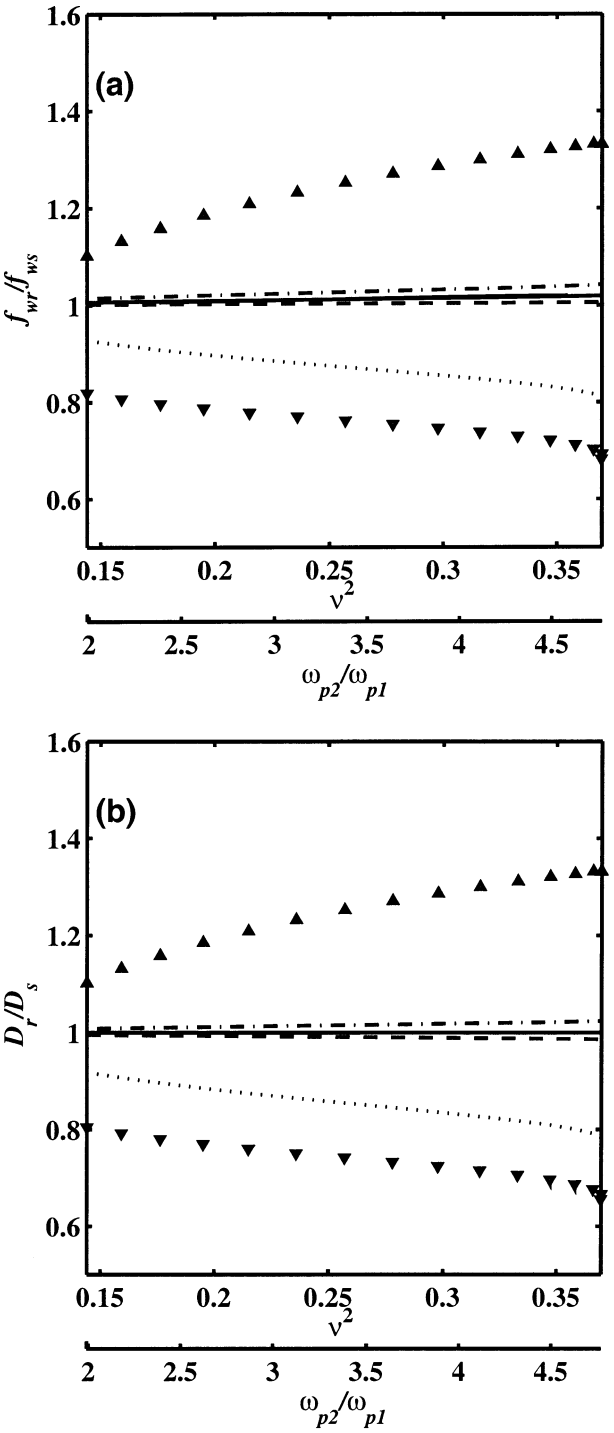

FIG. 3. (a) Normalized friction factor f_{wr}/f_{ws} and (b) total wave bottom dissipation D_r/D_s as a function of the spectral bandwidth υ^2 and the wave peak frequency ratio ω_{p2}/ω_{p1} for a bimodal wave with two superimposed JONSWAP wave spectra at two peak frequencies, f_{p1} and f_{p2}, at a 10-m water depth. The lower peak frequency is fixed at $f_{p1} = 0.06$, the Phillips coefficient is $\alpha = 0.001$, the spectral bandwidth parameter is $\sigma = 0.08$, and the peak enhancement parameter is $\gamma = 7$. The relative roughness r/A_r is 10^{-1}. Lines and symbols are as in Fig. 1.

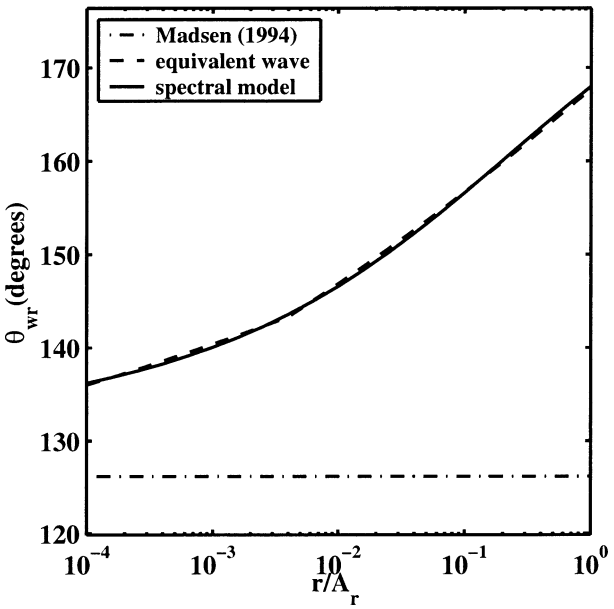

FIG. 4. Representative direction of wave bottom velocity as a function of relative roughness for a bidirectional and bimodal wave described by (3.3) and Fig. 2a, with a wave peak frequency ratio of $\omega_{p2}/\omega_{p1} = 3$ at a 10-m water depth and a current incident at 45° relative to the vector mean direction of the wave bottom velocity. Solid line is the spectral model, dashed line is the present model, and dash–dot line is the previous model by Madsen (1994).

bottom velocity spectra may come into existence in extremely shallow water, mixed swell and sea, and waves under a fast-turning wind field (cf. Weber 1991b).

According to Madsen's (1994) Taylor expansion method, the vector mean direction of the bottom stress is the same as that of the bottom velocity. According to the present theory, however, the former deviates significantly from the latter for a bidirectional, bimodal wave (Fig. 4). This deviation is likely to contribute to the mismatch of the wave directions and sand ripple directions observed by morphologists since the latter tend to orient along the vector mean direction of bottom stress.

All of the models we have discussed so far are based on the eddy viscosity model of the wave bottom boundary layer. Comparisons between the predicted bottom friction by the eddy viscosity model and other more sophisticated models with observations are given by Fredsoe and Deigard (1992) and Zou (2002). Moreover, we have assumed a known relative roughness in this paper. Thus, the relevance of the present model for practical wave models may be limited by the large uncertainty of the bottom roughness model for mobile beds (Nielsen 1992; Tolman 1994) as well as the inherent error of the eddy viscosity model (Fredsoe and Deigard 1992; Zou 2002).

Acknowledgments. The author thanks Drs. Alex Hay and Anthony Bowen for suggesting several improvements to the manuscript. The author is also grateful to

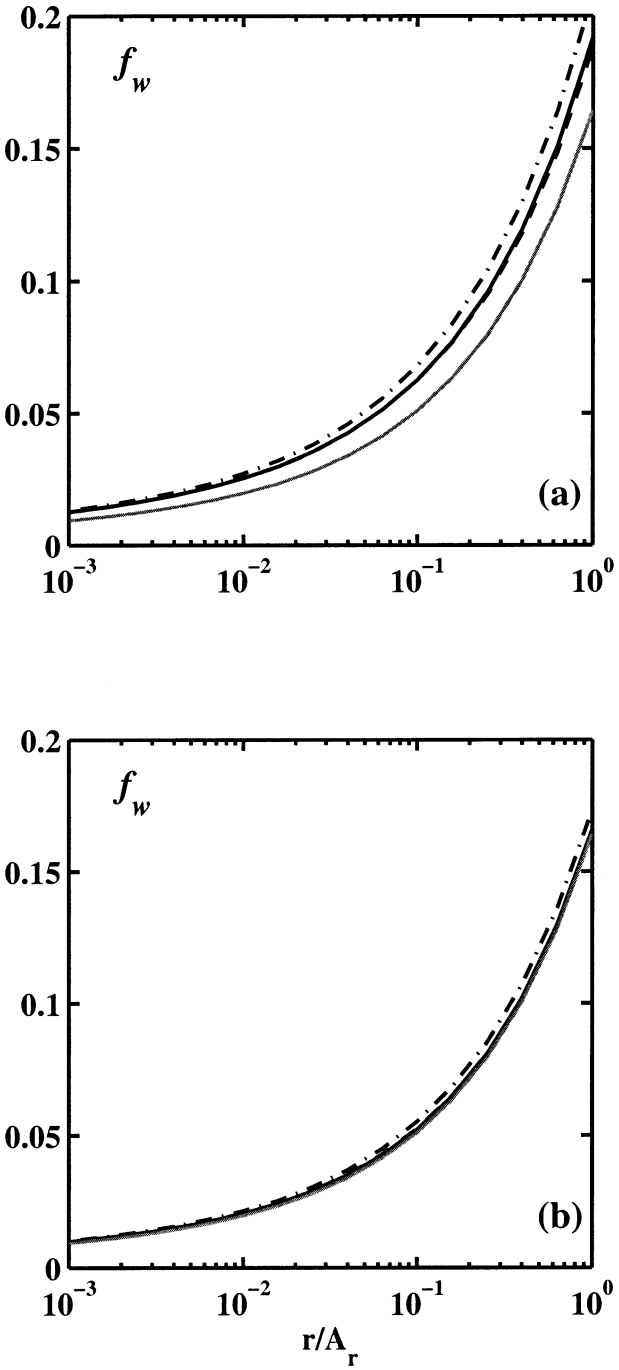

FIG. 5. Same as Fig. 4, but for wave bottom friction factor as a function of relative roughness: the current-to-wave friction velocity ratio, u_{*c}/u_{*w}, is (a) 1 and (b) 0.4; spectral model (solid line), present model (dashed line), previous model by Madsen (1994) (dash–dot line), and spectral model without current (gray line).

Dr. Will Perrie for discussions on finite-water-depth wave spectra and comments to improve the manuscript. The author thanks anonymous reviewers whose remarks contributed significantly to the manuscript. This research was funded by the Coastal Sciences Program of the U.S. Office of Naval Research, the Natural Science & Engineering Research Council of Canada, and the Petroleum Research Atlantic Canada (PRAC).

APPENDIX

The Transfer Function between Bottom Stress and Bottom Velocity

The transfer function between bottom stress and bottom velocity is related to the friction factor by [cf. (30) of Madsen 1994]

$$|T(\zeta_{0r})|^2 = (2\kappa^2)^{-1} f_{wr}. \tag{A.1}$$

The following approximation has been proposed for a monochromatic wave,

$$f_{wr} = C\left(\frac{r}{A_r}\right)^n, \tag{A.2}$$

where $C = 0.4$, $n = 3/4$ for $r/A_r > 0.02$ by Kamphuis (1974), and $C = 0.04$, $n = 1/4$ for $r/A_r < 0.02$ by Fredsoe and Deigard (1992).

Eliminating r/A_r from (A.1) and (A.2) yields

$$f_{wr} = C^{1/(1-n/2)}\left(\frac{30\kappa}{\sqrt{2}}\zeta_{0r}\right)^{n/(1-n/2)} \tag{A.3}$$

and, substituting (A.3) into (A.1), we have

$$|T(\zeta_{0r})|^2 = C_\zeta \zeta_{0r}^q, \tag{A.4}$$

where $C_\zeta = [2 \times 30^n \kappa^{2(1-n)} C^{-1}]^{1/(1-n/2)}$ and $q = n/(1 - n/2) = 0.3$ and 1.2 for $r/A_r < 0.02$ and $r/A_r > 0.02$.

REFERENCES

Ardhuin, F., T. H. C. Herbers, and W. C. O'Reilly, 2001: A hybrid Eulerian–Lagrangian model for spectral wave evolution with application to bottom friction on the continental shelf. *J. Phys. Oceanogr.,* **31,** 1498–1516.

Bouws, E., H. Gunther, W. Rosenthal, and C. L. Vincent, 1985: Similarity of the wind wave spectrum in finite depth water. *J. Geophys. Res.,* **90** (C1), 975–986.

Christoffersen, J. B., and I. G. Jonsson, 1985: Bed friction and dissipation in a combined current and wave motion. *Ocean Eng.,* **12** (5), 387–423.

Collins, J. I., 1972: Prediction of shallow water spectra. *J. Geophys. Res.,* **77,** 2693–2707.

Fredsoe, J., and R. Deigaard, 1992: *Mechanics of Coastal Sediment Transport.* World Scientific, 369 pp.

Graber, H. C., 1984: A parametric wind wave model for arbitrary water depths. Sc.D. thesis, Massachusetts Institute of Technology, 310 pp.

Grant, W. D., and O. S. Madsen, 1979: Combined wave and current interaction with rough bottom. *J. Geophys. Res.,* **84,** 1797–1808.

Hasselmann, K., and I. I. Collins, 1968: Spectral wave dissipation of finite depth gravity waves due to turbulent bottom friction. *J. Mar. Res.,* **26,** 1–12.

Kajiura, K., 1968: A model of the bottom boundary layer in water waves. *Bull. Earthquake Res. Inst.,* **46,** 75–123.

Kamphuis, J. W., 1974: Friction factors under oscillatory waves. *J. Waterw. Port Coastal Eng. Div.,* **101** (WW2), 135–144.

Longuet-Higgins, M. S., 1983: On the joint distribution of wave pe-

riods and amplitudes in a random wave field. *Proc. Roy. Soc. London*, **A389,** 241–258.
Madsen, O. S., 1994: Spectral wave-current bottom boundary layer flows. *Proc. ASCE 24th Int. Conf. on Coastal Engineering (ICCE)*, Kobe, Japan, ASCE, 384–398.
——, Y.-K. Poon, and H. C. Graber, 1988: Spectral wave attenuation by bottom friction: Theory. *Proc. ASCE 21st Int. Conf. on Coastal Engineering (ICCE)*, Malaga, Spain, ASCE, 492–504.
Mathisen, P. P., and O. S. Madsen, 1999: Waves and currents over a fixed rippled bed. Part 3: Bottom and apparent roughness for spectral waves and currents. *J. Geophys. Res.*, **104** (C8), 18 447–18 461.
Nielsen, P., 1992: *Coastal Bottom Boundary Layers and Sediment Transport.* World Scientific, 324 pp.
Tolman, H. L., 1994: Wind waves and moveable-bed bottom friction. *J. Phys. Oceanogr.*, **24,** 994–1009.
Weber, S. L., 1991a: Bottom friction for wind sea and swell in extreme depth-limited situations. *J. Phys. Oceanogr.*, **21,** 149–172.
——, 1991b: Eddy-viscosity and drag-law models for random ocean wave dissipation. *J. Fluid Mech.*, **232,** 73–98.
Young, I. R., and R. M. Gorman, 1995: Measurements of the evolution of ocean wave spectra due to bottom friction. *J. Geophys. Res.*, **100** (C6), 10 987–11 004.
Zou, Q.-P., 2002: An analytical model of wave bottom boundary layers incorporating turbulent relaxation and diffusion effects. *J. Phys. Oceanogr.*, **32,** 2441–2456.